



TITLE:

Perivascular leukocyte clusters are essential for efficient activation of effector T cells in the skin.

AUTHOR(S):

Natsuaki, Yohei; Egawa, Gyohei; Nakamizo, Satoshi; Ono, Sachiko; Hanakawa, Sho; Okada, Takaharu; Kusuba, Nobuhiro; ... Guttman-Yassky, Emma; Miyachi, Yoshiki; Kabashima, Kenji

CITATION:

Natsuaki, Yohei ...[et al]. Perivascular leukocyte clusters are essential for efficient activation of effector T cells in the skin.. Nature immunology 2014, 15: 1064-1069

ISSUE DATE:

2014-09-21

URL:

<http://hdl.handle.net/2433/189891>

RIGHT:

© 2014 Nature America, Inc.; 許諾条件により本文は2015-03-22に公開;
This is not the published version. Please cite only the published
version.; この論文は出版社版ではありません。引用の際には出版社版を
ご確認ご利用ください。

Perivascular leukocyte clusters are essential for efficient effector T cell activation in the skin

Yohei Natsuaki^{1,13,15}, Gyohei Egawa^{1,15}, Satoshi Nakamizo¹, Sachiko Ono¹, Sho Hanakawa¹, Takaharu Okada², Nobuhiro Kusuba¹, Atsushi Otsuka¹, Akihiko Kitoh¹, Tetsuya Honda¹, Saeko Nakajima¹, Soken Tsuchiya³, Yukihiro Sugimoto³, Ken J. Ishii^{4,5}, Hiroko Tsutsui⁶, Hideo Yagita⁷, Yoichiro Iwakura^{8,9}, Masato Kubo^{10,11}, Lai guan Ng¹², Takashi Hashimoto¹³, Judilyn Fuentes¹⁴, Emma Guttman-Yassky¹⁴, Yoshiki Miyachi¹, and Kenji Kabashima¹

¹ Department of Dermatology, Kyoto University Graduate School of Medicine, Kyoto, Japan.

² Research Unit for Immunodynamics, RIKEN Research Center for Allergy and Immunology, Kanagawa, Japan.

³ Department of Pharmaceutical Biochemistry, Graduate School of Pharmaceutical Sciences, Kumamoto University, Kumamoto, Japan.

⁴ Laboratory of Adjuvant Innovation, National Institute of Biomedical Innovation, Osaka, Japan.

⁵ Laboratory of Vaccine Science, WPI Immunology Frontier Research Center (iFReC), Osaka University, Osaka, Japan.

⁶ Departments of Microbiology, Hyogo College of Medicine, Hyogo, Japan.

⁷ Department of Immunology, Juntendo University School of Medicine, Tokyo, Japan.

⁸ Research Institute for Biomedical Sciences, Tokyo University of Science, Chiba, Japan

⁹ Medical Mycology Research Center, Chiba University, Chiba, Japan

¹⁰ Laboratory for Cytokine Regulation, RIKEN center for Integrative Medical Science (IMS), Kanagawa, Japan.

¹¹ Division of Molecular Pathology, Research Institute for Biomedical Science, Tokyo University of Science, Chiba, Japan

¹² Singapore Immunology Network (SIgN), A*STAR (Agency for Science, Technology and Research), Biopolis, Singapore

¹³ Department of Dermatology, Kurume University School of Medicine, Fukuoka, Japan.

¹⁴ Department of Dermatology, Icahn School of Medicine at Mount Sinai School Medical Center, New York, NY.

¹⁵ These authors contributed equally to this work.

- 35 Correspondence to Kenji Kabashima, MD, PhD
36 Department of Dermatology, Kyoto University Graduate School of Medicine
37 54 Shogoin-Kawahara, Kyoto 606-8507, Japan
38 Phone: +81-75-751-3605; Fax: +81-75-761-3002
39 E-mail: kaba@kuhp.kyoto-u.ac.jp
40

41 It remains largely unclear how antigen-presenting cells encounter effector or memory T cells
42 efficiently in the periphery. Here we used a murine contact hypersensitivity model and
43 showed that upon epicutaneous antigen challenge, dendritic cells (DCs) formed clusters with
44 effector T cells in dermal perivascular areas to promote *in situ* proliferation and activation of
45 skin T cells in an antigen- and integrin LFA-1-dependent manner. We found that DCs
46 accumulated in perivascular areas and DC clustering was abrogated by macrophage-depletion.
47 Interleukin 1 α (IL-1 α) treatment induced the production of the chemokine CXCL2 from
48 dermal macrophages, and DC clustering was suppressed by blockade of either IL-1 receptor
49 (IL-1R) or CXCR2, the receptor for CXCL2. These findings suggest that dermal leukocyte
50 cluster is an essential structure for elicitation of the acquired cutaneous immunity.

51

Boundary tissues, including the skin, are continually exposed to foreign antigens, which must be monitored and possibly eliminated. Upon foreign antigen exposure, skin dendritic cells (DCs), including epidermal Langerhans cells (LCs), capture the antigens and migrate to draining lymph nodes (LNs) where antigen presentation to naïve T cells occurs mainly in the T cell zone. In this location naïve T cells accumulation in the vicinity of DCs is mediated by CCR7 signaling¹. The T cell zone in the draining LNs facilitates the efficient encounter of antigen-bearing DCs with antigen-specific naïve T cells.

As opposed to LNs, the majority of skin T cells, including infiltrating skin T cells and skin resident T cells, have an effector-memory phenotype². In addition, antigen presentation to skin T cells by antigen-presenting cells (APCs) is the crucial step in elicitation of acquired skin immune responses, such as contact dermatitis. Therefore, we hypothesize that antigen-presentation in the skin should be substantially different from that in LNs. Previous studies using murine contact hypersensitivity (CHS), as a model of human contact dermatitis, have revealed that dermal DCs (dDCs), but not epidermal LCs, have a pivotal role in the transport and presentation of antigen to the LNs³. In the skin, however, it remains unclear which subset of APCs presents antigens to skin T cells, and how skin T cells efficiently encounter APCs. In addition, dermal macrophages are key modulators in CHS response⁴, but the precise mechanisms by which macrophages are involved in antigen recognition in the skin have not yet been clarified. These unsolved questions prompted us to focus where skin T cells recognize antigens and how skin T cells are activated in the elicitation phase of acquired cutaneous immune responses, such as CHS.

When keratinocytes encounter foreign antigens, they immediately produce various pro-inflammatory mediators such as interleukin 1 (IL-1) and tumor necrosis factor (TNF) in an antigen-nonspecific manner^{5, 6}. IL-1 family proteins are considered important modulators in CHS responses, because hapten-specific T cell activation was shown to be impaired in IL-1 α and IL-1 β -deficient mice, but not in TNF-deficient mice⁷. IL-1 α and IL-1 β are agonistic ligands of the IL-1 receptor (IL-1R). While IL-1 α is stored in keratinocytes and secreted upon exposure to nonspecific stimuli, IL-1 β is produced mainly by epidermal LCs and dermal mast cells in an inflammasome-dependent manner via NALP3 and caspase 1/11 activation. Because these pro-inflammatory mediators are crucial in the initiation of acquired immune responses such as CHS, it is of great interest to understand how IL-1 modulates antigen recognition by skin T cells.

Using a murine CHS model, here we examined how DCs and effector T cells encounter

each other efficiently in the skin. We found that upon encounter with antigenic stimuli dDCs formed clusters in which effector T cells were activated and proliferated in an antigen-dependent manner. These DC–T cell clusters were initiated by skin macrophages via IL-1R signaling and were essential for the establishment of cutaneous acquired immune responses.

RESULTS

DC–T cell clusters are formed at antigen-challenged sites

To explore immune cell accumulation in the skin, we examined the clinical and histological features of elicitation of human allergic contact dermatitis. Allergic contact dermatitis is the most common of eczematous skin diseases, affecting 15–20% of the general population worldwide⁸, and is mediated by T cells. Although antigens may be applied relatively evenly over the surface of skin, clinical manifestations commonly include discretely distributed small vesicles (**Fig. 1a**), suggesting an uneven occurrence of intense inflammation. Histological examination of allergic contact dermatitis showed spongiosis, intercellular edema in the epidermis and co-localization of perivascular infiltrates of CD3⁺ T cells and spotty accumulation of CD11c⁺ DCs in the dermis, especially beneath the vesicles (**Fig. 1b**). These findings led us to hypothesize that focal accumulation of T cells and DCs in the dermis may contribute to vesicle formation in early eczema.

To characterize the DC–T cell clusters in elicitation reactions, we obtained time-lapse images in a murine model of CHS using two-photon microscopy. T cells were isolated from the draining LNs of 2, 4-dinitrofluorobenzene (DNFB)-sensitized mice, labeled and transferred into CD11c-yellow fluorescent protein (YFP) mice. In the steady state, YFP⁺ dDCs distributed diffusely (**Fig. 1c**), representing nondirected movement in a random fashion, as reported previously (**Supplementary Fig. 1**). After topical challenge with DNFB, YFP⁺ dDCs transiently increased their velocities and formed clusters in the dermis, with the clusters becoming larger and more evident after 24 h (**Fig. 1c** and **Supplementary Movie 1**). At the same time, transferred T cells accumulated in the DC clusters and interacted with YFP⁺ DCs for several hours (**Fig. 1d** and **Supplementary Movie 2**). Thus, the accumulation of DCs and T cells in the dermis is observed in mice during CHS responses. We observed that the intercellular spaces between keratinocytes overlying the DC–T cell clusters in the dermis were enlarged (**Fig. 1e**), replicating observations in human allergic contact dermatitis (**Fig. 1b**).

We next sought to determine which of the two major DC populations in skin, epidermal LCs or dDCs, were essential for the elicitation of CHS. To deplete all cutaneous DC subsets, Langerin-diphtheria toxin receptor (DTR) mice were transferred with bone marrow (BM) cells from CD11c-DTR mice. To selectively deplete LCs or dDCs, Langerin-DTR or C57BL/6 mice were transferred with BM cells from C57BL/6 mice or CD11c-DTR mice, respectively (**Supplementary Fig. 2a, b**). We injected diphtheria toxin (DT) for depletion of each DC subset before elicitation and found that ear swelling and inflammatory histological findings were significantly attenuated in the absence of dDCs, but not in the absence of LCs (**Fig. 1f** and **Supplementary Fig. 2c**). In addition, interferon (IFN)- γ production in skin T cells was strongly suppressed in dDC-depleted mice (**Fig. 1g**). These results suggest that dDCs, and not epidermal LCs, are essential for T cell activation and the elicitation of CHS responses.

Skin effector T cells proliferate *in situ* in an antigen-dependent manner

To evaluate the impact of DC–T cell clusters in the dermis, we determined whether T cells had acquired the ability to proliferate via DC–T cell accumulation in the dermis. CD4⁺ or CD8⁺ T cells purified from the draining LNs of DNFB-sensitized mice were labeled with CellTraceTM Violet and transferred into naïve mice. Twenty-four hours after DNFB application, we collected the skin to evaluate T cell proliferation by dilution of fluorescent intensity. The majority of infiltrating T cells were CD44⁺ CD62L⁺ effector T cells (**Supplementary Fig. 2d**). Among the infiltrating T cells, CD8⁺ T cells proliferated actively, whereas the CD4⁺ T cells showed low proliferative potency (**Fig. 2a**). This T cell proliferation was antigen-dependent, because 2,4,6-trinitrochlorobenzene (TNCB)-sensitized T cells exhibited low proliferative activities in response to DNFB application (**Fig. 2a**). In line with this finding, the DC–T cell conjugation time was prolonged in the presence of cognate antigens (**Fig. 2b**), and the T cells interacting with DCs within DC–T cell clusters proliferated (**Fig. 2c** and **Supplementary Movie 3**). Our findings indicate that skin effector T cells conjugate with DCs and proliferate *in situ* in an antigen-dependent manner.

CD8⁺ T cell activation in DC–T cell clusters is LFA-1 dependent

A sustained interaction between DCs and naïve T cells, which is known as an immunological synapse, is maintained by cell adhesion molecules⁹. Particularly, the integrin LFA-1 on T cells binds to cell surface glycoproteins, such as intercellular adhesion molecule-1 (ICAM-1),

on APCs, which is essential for naïve T cell proliferation and activation during antigen recognition in the LNs. To examine whether LFA-1-ICAM-1 interactions are required for effector T cell activation in DC–T cell clusters in the skin, an anti-LFA-1 neutralizing antibody, KBA, was intravenously injected 14 h after elicitation with DNFB in CHS. KBA administration reduced T cells accumulation in the dermis (**Fig. 3a**). The velocity of T cells in the cluster was $0.65 \pm 0.29 \mu\text{m}/\text{min}$ 14 h after DNFB challenge and increased up to 3-fold ($1.64 \pm 1.54 \mu\text{m}/\text{min}$) at 8 h after treatment with KBA, while it was not affected by treatment with an isotype-matched control IgG (**Fig. 3b**). At the outside of clusters, T cells smoothly migrated at the mean velocity of $2.95 \pm 1.19 \mu\text{m}/\text{min}$, consistent with previous results¹⁰, and was not affected by control-IgG treatment (data not shown). Treatment with KBA also attenuated ear swelling significantly (**Fig. 3c**), as well as IFN- γ production by skin CD8⁺ T cells (**Fig. 3d, e**). These results suggest that DC–effector T cell conjugates are integrin-dependent, similar to the DC–naïve T cell interactions in draining LNs.

Skin macrophages are required for dDC clustering

We next examined the initiation factors of DC–T cell accumulation. dDC clusters were also formed in response to the initial application of hapten (sensitization phase), but their number was significantly decreased 48 h after sensitization, while DC clusters persisted for 48 h in the elicitation phase (**Fig. 4a and Supplementary Fig. 3a**). These DC clusters were abrogated 7 days after DNFB application (data not shown). These observations suggest that DC–T cell accumulation is initiated by DC clustering, which then induces the accumulation, proliferation and activation of T cells, a process that depends on the presence of antigen-specific effector T cells *in situ*. DC clusters were also induced by solvents such as acetone or adjuvants such as dibutylphthalic acid and *Mycobacterium bovis* BCG-inoculation (**Supplementary Fig. 3b, c**). In addition, DC clusters were observed not only in the ear skin, but also in other regions such as the back skin and the footpad (**Supplementary Fig. 3d**). These results suggest that DC cluster formation is not an ear-specific event, but a general mechanism during skin inflammation.

The initial DC clusters were not decreased in recombination activating gene 2 (RAG2)-deficient mice, in which T and B cells are absent, in lymphoid tissue inducer cell-deficient *aly/aly* mice¹¹ or in mast cell or basophil-depleted mice, using MasTRECK or BasTRECK mice^{12, 13} (**Fig. 4b**). In contrast, DC clusters were abrogated in C57BL/6 mice transferred with BM from LysM-DTR mice, in which both macrophages and neutrophils

were depleted by treatment with DT (**Fig. 4b, c**). The depletion of neutrophils alone, by administration of anti-Ly6G antibody (1A8), did not interfere with DC cluster formation (**Fig. 4b**), which suggested that macrophages, but not neutrophils, were required during the formation of DC clusters. Of note, DC cluster formation was not attenuated by anti-LFA-1 neutralizing KBA antibody treatment (**Supplementary Fig. 3e, f**), suggesting that macrophages-DCs interaction were LFA-1-independent. Consistent with the DC cluster formation, the elicitation of the CHS response (**Fig. 4d**) and IFN- γ production by skin T cells (**Fig. 4e**) were significantly suppressed in LysM-DTR BM chimeric mice treated with DT. Thus, skin macrophages were required for formation of DC clusters, which was necessary for T cell activation and the elicitation of CHS.

Macrophages are required for perivascular DCs clustering

To examine the kinetics of dermal macrophage and DCs *in vivo*, we visualized them by two-photon microscopy. *In vivo* labeling of blood vessels with tetramethylrhodamine isothiocyanate (TRITC)-conjugated dextran revealed that dDCs distributed diffusely in the steady state (**Fig. 5a, left**). After hapten-application to the ear of previously sensitized mice, dDCs accumulated mainly around post-capillary venules (**Fig. 5a, right** and **Fig. 5b**). Time-lapse imaging revealed that some of dDCs showed directional migration toward TRITC-positive cells that were labeled red by incorporating extravasated TRITC-dextran (**Fig. 5c and Supplementary Movie 4**). The majority of TRITC-positive cells were F4/80⁺ CD11b⁺ macrophages (**Supplementary Fig. 4a**). These observations prompted us to examine the role of macrophages in DC accumulation. We used a chemotaxis assay to determine whether macrophages attracted the DCs. dDCs and dermal macrophages were isolated from dermal skin cell suspensions and incubated in a transwell assay for 12 h. dDCs placed in the upper wells efficiently migrated to the lower wells that contain dermal macrophages (**Fig. 5d**). But this dDC migration was not observed when macrophages were absent in the lower wells (**Fig. 5d**). Thus, dermal macrophages have a capacity to attract dDCs *in vitro*, which may lead to dDC accumulation around post-capillary venules.

IL-1 α is required for DC cluster formation upon antigen challenge

We attempted to explore the underlying mechanism of DC cluster formation. We observed that DC accumulation occurred during the first application of hapten (**Fig. 4a**), which suggested that an antigen-nonspecific mechanism, such as production of the

pro-inflammatory mediator IL-1, may initiate DC clustering. Hapten-induced DC accumulation was not decreased in NALP3- or caspase-1-11-deficient mice, but was decreased significantly in IL-1R1-deficient mice, which lack a receptor for IL-1 α , IL-1 β , and IL-1R antagonist, or after the subcutaneous administration of an IL-1R antagonist (**Fig. 6a,b**). Consistent with these observations, the elicitation of CHS and IFN- γ production by skin T cells were significantly attenuated in mice that lack both IL-1 α and IL-1 β (**Fig. 6c, d**). In addition, the formation of dDC clusters was suppressed significantly by the subcutaneous injection of an anti-IL-1 α neutralizing antibody, but only marginally by an anti-IL-1 β neutralizing antibody (**Fig. 6b**). Because keratinocytes are known to produce IL-1 α upon hapten application¹⁴, our results suggest that IL-1 α has a major role in mediating the formation of DC clustering.

M2 macrophages produce CXCL2 to attract dDCs

To further characterize how macrophages attract dDCs, we examined *Il1r1* expression in BM-derived M1 and M2 macrophages, classified as such based on the differential mRNA expression of *Tnf*, *Nos2*, *Il12a*, *Arg1*, *Retnla* and *Chi3l3* (**Supplementary Fig. 4b**)¹⁵. We found that M2 macrophages had higher expression of *Il1r1* mRNA compared to M1 macrophages (**Fig. 6e**). We also found that the subcutaneous injection of pertussis toxin, a inhibitory regulative G protein (Gi)-specific inhibitor, almost completely abrogated DC cluster formation in response to hapten-stimuli (**Fig. 6b**) suggesting that signaling through Gi-coupled chemokines was required for DC cluster formation.

We next used microarrays to examine the effect of IL-1 α on the expression of chemokines in M1 and M2 macrophages. IL-1 α treatment did not enhance chemokine expression in M1 macrophages, whereas it increased *Ccl5*, *Ccl17*, *Ccl22* and *Cxcl2* mRNA expression in M2 macrophages (**Supplementary Table 1**). Among them, *Cxcl2* expression was enhanced most prominently by treatment with IL-1 α , a result validated by real-time polymerase chain reaction (PCR) analysis (**Fig. 6f**). Consistently, *Cxcl2* mRNA expression was significantly increased in DNFB-painted skin (**Supplementary Fig. 5a**) and was not affected by neutrophil depletion with 1A8 (**Supplementary Fig. 5b, c**). In addition, IL-1 α -treated dermal macrophages produced *Cxcl2* mRNA *in vitro* (**Supplementary Fig. 5d**). These results suggest that dermal macrophages, but not neutrophils, are the major source of CXCL2 during CHS. We also detected high expression of the mRNA for *Cxcr2*, the receptor for CXCL2, in DCs (**Supplementary Fig. 5e**), which prompted us to examine the role of CXCR2 on dDCs.

The formation of DC clusters in response to hapten stimuli was substantially reduced by the intraperitoneal administration of the CXCR2 inhibitor SB265610¹⁶ (**Fig. 6g**). In addition, SB265610-treatment during the elicitation of CHS inhibited ear swelling (**Fig. 6h**) and IFN- γ production by skin T cells (**Fig. 6i**).

Taken together, in the absence of effector T cells specific for a cognate antigen (i.e. in the sensitization phase of CHS), DC clustering is a transient event, and hapten-carrying DCs migrate into draining LNs to establish sensitization. On the other hand, in the presence of the antigen and antigen-specific effector or memory T cells, DC clustering is followed by T cell accumulation (i.e. in the elicitation phase of CHS) (**Supplementary Fig. 6**). Thus, dermal macrophages are essential for initiating DC cluster formation through the production of CXCL2, and that DC clustering plays an important role for efficient activation of skin T cells.

DISCUSSION

Although the mechanistic events in the sensitization phase in cutaneous immunity have been studied thoroughly over 20 years^{17, 18}, what types of immunological events occur during the elicitation phases in the skin has remained unclear. Here we describe the antigen-dependent induction of DC and T cell clusters in the skin in a murine model of CHS and show that effector T cells-DCs interactions in these clusters are required to induce efficient antigen-specific immune responses in the skin. We show that dDCs, but not epidermal LCs, are essential for antigen presentation to skin effector T cells and they exhibit sustained association with effector T cells in an antigen- and LFA-1-dependent manner. IL-1 α , and not the inflammasome, initiates the formation of these perivascular DC clusters.

Epidermal contact with antigens triggers release of IL-1 in the skin¹⁴. Previous studies have shown that the epidermal keratinocytes constitute a major reservoir of IL-1 α ⁶ and mechanical stress to keratinocytes permits release of large amounts of IL-1 α even in the absence of cell death¹⁹. The cellular source of IL-1 α in this process remains unclear. We show that IL-1 α activates macrophages that subsequently attract dDCs, mainly to areas around post-capillary venules, where effector T cells are known to transmigrate from the blood into the skin²⁰. In the presence of the antigen and antigen-specific effector T cells, DC clustering is followed by T cell accumulation. Therefore, we propose that these perivascular dDC clusters may provide antigen-presentation sites for efficient effector T cell activation. This is suggested by the observations that CHS responses and intracutaneous T cell activation were attenuated

significantly in the absence of these clusters, in condition of macrophage depletion or inhibiting integrin functions, IL-1R signaling^{21, 22} or CXCR2 signaling²³.

In contrast to the skin, antigen presentations in other peripheral barrier tissues is relatively well understood. In submucosal areas, specific sentinel lymphoid structures called mucosa-associated lymphoid tissue (MALT), serve as peripheral antigen presentation sites²⁴, and lymphoid follicles are present in the normal bronchi (bronchus-associated lymphoid tissue; BALT). These structures serve as antigen presentation sites in non-lymphoid peripheral organs. By analogy, the concept of skin-associated lymphoid tissue (SALT) was proposed in the early 1980's, based on findings that cells in the skin are capable of capturing, processing and presenting antigens^{25, 26}. However, the role of cellular skin components as antigen presentation sites has remained uncertain. Here we have identified an inducible structure formed by dermal macrophages, dDCs and effector T cells, which seem to accumulate sequentially. Because formation of this structure is essential for efficient effector T cell activation, these inducible leukocyte clusters may function as SALTs. Unlike MALTs, these leukocyte clusters are not found at steady state, but are induced during the development of an adaptive immune response. Therefore, these clusters may be better named as inducible SALTs (iSALT), similar to inducible BALTs (iBALT) in the lung²⁷. In contrast to iBALTs, we could not identify naïve T cells or B cells in SALTs (data not shown), suggesting that the leukocyte clusters in the skin may be specialized for effector T cell activation but not for naïve T cell activation. Our findings suggest that approaches to the selective inhibition of this structure may have novel therapeutic benefit in inflammatory disorders of the skin.

ACKNOWLEDGEMENTS

We thank Dr. P. Bergstresser and Dr. J. Cyster for critical reading of our manuscript. This work was supported in part by Grants-in-Aid for Scientific Research from the Ministry of Education, Culture, Sports, Science and Technology of Japan.

AUTHOR CONTRIBUTIONS

Y.N., G.E., and K.K designed this study and wrote the manuscript. Y.N., G.E, S.N., S.O., S.H., N.K., A.O., A.K., T.H., and S.N. performed the experiments and data analysis. S.T. and Y.S. did experiments related to microarray analysis. J.F. and E. G-Y did experiments related to immunohistochemistry of human samples. K.J.I, H.T., H. Y, Y. I., L.G.N., and M.K.

318 developed experimental reagents and gene-targeted mice. T.O., Y.M., and K.K. directed the
319 project and edited the manuscript. All authors reviewed and discussed the manuscript.

320

321

322 **COMPETING FINANCIAL INTERESTS**

323 The authors declare no competing financial interests.

324

325

326 **ACCESSION CODES**

327 Microarray data have been deposited in NCBI-GEO under accession number GSE53680.

328

329

REFERENCES

1. von Andrian UH, Mempel TR. Homing and cellular traffic in lymph nodes. *Nat Rev Immunol* 2003, **3**(11): 867-878.
2. Clark RA, Chong B, Mirchandani N, Brinster NK, Yamanaka K, Dowgiert RK, *et al.* The vast majority of CLA+ T cells are resident in normal skin. *J Immunol* 2006, **176**(7): 4431-4439.
3. Wang L, Bursch LS, Kissenpfennig A, Malissen B, Jameson SC, Hogquist KA. Langerin expressing cells promote skin immune responses under defined conditions. *J Immunol* 2008, **180**(7): 4722-4727.
4. Tuckermann JP, Kleiman A, Moriggl R, Spanbroek R, Neumann A, Illing A, *et al.* Macrophages and neutrophils are the targets for immune suppression by glucocorticoids in contact allergy. *J Clin Invest* 2007, **117**(5): 1381-1390.
5. Sims JE, Smith DE. The IL-1 family: regulators of immunity. *Nat Rev Immunol* 2010, **10**(2): 89-102.
6. Murphy JE, Robert C, Kupper TS. Interleukin-1 and cutaneous inflammation: a crucial link between innate and acquired immunity. *J Invest Dermatol* 2000, **114**(3): 602-608.
7. Nakae S, Komiyama Y, Narumi S, Sudo K, Horai R, Tagawa Y, *et al.* IL-1-induced tumor necrosis factor-alpha elicits inflammatory cell infiltration in the skin by inducing IFN-gamma-inducible protein 10 in the elicitation phase of the contact hypersensitivity response. *Int Immunol* 2003, **15**(2): 251-260.
8. Thyssen JP, Linneberg A, Menne T, Nielsen NH, Johansen JD. Contact allergy to allergens of the TRUE-test (panels 1 and 2) has decreased modestly in the general population. *Br J Dermatol* 2009, **161**(5): 1124-1129.
9. Springer TA, Dustin ML. Integrin inside-out signaling and the immunological synapse. *Curr Opin Cell Biol* 2012, **24**(1): 107-115.

10. Egawa G, Honda T, Tanizaki H, Doi H, Miyachi Y, Kabashima K. In vivo imaging of T-cell motility in the elicitation phase of contact hypersensitivity using two-photon microscopy. *J Invest Dermatol* 2011, **131**(4): 977-979.
11. Miyawaki S, Nakamura Y, Suzuka H, Koba M, Yasumizu R, Ikehara S, *et al.* A new mutation, *aly*, that induces a generalized lack of lymph nodes accompanied by immunodeficiency in mice. *Eur J Immunol* 1994, **24**(2): 429-434.
12. Sawaguchi M, Tanaka S, Nakatani Y, Harada Y, Mukai K, Matsunaga Y, *et al.* Role of mast cells and basophils in IgE responses and in allergic airway hyperresponsiveness. *J Immunol* 2012, **188**(4): 1809-1818.
13. Otsuka A, Kubo M, Honda T, Egawa G, Nakajima S, Tanizaki H, *et al.* Requirement of interaction between mast cells and skin dendritic cells to establish contact hypersensitivity. *PLoS One* 2011, **6**(9): e25538.
14. Enk AH, Katz SI. Early molecular events in the induction phase of contact sensitivity. *Proc Natl Acad Sci U S A* 1992, **89**(4): 1398-1402.
15. Weissner SB, McLaren KW, Kuroda E, Sly LM. Generation and characterization of murine alternatively activated macrophages. *Methods Mol Biol* 2013, **946**: 225-239.
16. Liao L, Ning Q, Li Y, Wang W, Wang A, Wei W, *et al.* CXCR2 blockade reduces radical formation in hyperoxia-exposed newborn rat lung. *Pediatr Res* 2006, **60**(3): 299-303.
17. Honda T, Egawa G, Grabbe S, Kabashima K. Update of immune events in the murine contact hypersensitivity model: toward the understanding of allergic contact dermatitis. *J Invest Dermatol* 2013, **133**(2): 303-315.
18. Kaplan DH, Igyarto BZ, Gaspari AA. Early immune events in the induction of allergic contact dermatitis. *Nat Rev Immunol* 2012, **12**(2): 114-124.

- 398 19. Lee RT, Briggs WH, Cheng GC, Rossiter HB, Libby P, Kupper T. Mechanical
399 deformation promotes secretion of IL-1 alpha and IL-1 receptor antagonist. *J Immunol*
400 1997, **159**(10): 5084-5088.
401
- 402 20. Sackstein R, Falanga V, Streilein JW, Chin YH. Lymphocyte adhesion to psoriatic
403 dermal endothelium is mediated by a tissue-specific receptor/ligand interaction. *J*
404 *Invest Dermatol* 1988, **91**(5): 423-428.
405
- 406 21. Kish DD, Gorbachev AV, Fairchild RL. IL-1 receptor signaling is required at multiple
407 stages of sensitization and elicitation of the contact hypersensitivity response. *J*
408 *Immunol* 2012, **188**(4): 1761-1771.
409
- 410 22. Kondo S, Pastore S, Fujisawa H, Shivji GM, McKenzie RC, Dinarello CA, *et al.*
411 Interleukin-1 receptor antagonist suppresses contact hypersensitivity. *J Invest*
412 *Dermatol* 1995, **105**(3).
413
- 414 23. Cattani F, Gallese A, Mosca M, Buanne P, Biordi L, Francavilla S, *et al.* The role of
415 CXCR2 activity in the contact hypersensitivity response in mice. *Eur Cytokine Netw*
416 2006, **17**(1): 42-48.
417
- 418 24. Brandtzaeg P, Kiyono H, Pabst R, Russell MW. Terminology: nomenclature of
419 mucosa-associated lymphoid tissue. *Mucosal Immunol* 2008, **1**(1): 31-37.
420
- 421 25. Streilein JW. Skin-associated lymphoid tissues (SALT): origins and functions. *J Invest*
422 *Dermatol* 1983, 80 Suppl: 12s-16s.
423
- 424 26. Egawa G, Kabashima K. Skin as a peripheral lymphoid organ: revisiting the concept
425 of skin-associated lymphoid tissues. *J Invest Dermatol* 2011, **131**(11): 2178-2185.
426
- 427 27. Moyron-Quiroz JE, Rangel-Moreno J, Kusser K, Hartson L, Sprague F, Goodrich S,
428 *et al.* Role of inducible bronchus associated lymphoid tissue (iBALT) in respiratory
429 immunity. *Nat med* 2004, **10**(9): 927-934.
430
- 431 28. Kissenpfennig A, Henri S, Dubois B, Laplace-Builhe C, Perrin P, Romani N, *et al.*

- 432 Dynamics and function of Langerhans cells in vivo: dermal dendritic cells colonize
- 433 lymph node areas distinct from slower migrating Langerhans cells. *Immunity* 2005,
- 434 **22(5):** 643-654.
- 435
- 436 29. Jung S, Unutmaz D, Wong P, Sano G, De los Santos K, Sparwasser T, *et al.* In vivo
- 437 depletion of CD11c+ dendritic cells abrogates priming of CD8+ T cells by exogenous
- 438 cell-associated antigens. *Immunity* 2002, **17(2):** 211-220.
- 439
- 440 30. Lindquist RL, Shakhar G, Dudziak D, Wardemann H, Eisenreich T, Dustin ML, *et al.*
- 441 Visualizing dendritic cell networks in vivo. *Nat immunol* 2004, **5(12):** 1243-1250.
- 442
- 443 31. Miyake Y, Kaise H, Isono K, Koseki H, Kohno K, Tanaka M. Protective role of
- 444 macrophages in noninflammatory lung injury caused by selective ablation of alveolar
- 445 epithelial type II Cells. *J Immunol* 2007, **178(8):** 5001-5009.
- 446
- 447 32. Hao Z, Rajewsky K. Homeostasis of peripheral B cells in the absence of B cell influx
- 448 from the bone marrow. *J Exp Med* 2001, **194(8):** 1151-1164.
- 449
- 450 33. Horai R, Asano M, Sudo K, Kanuka H, Suzuki M, Nishihara M, *et al.* Production of
- 451 mice deficient in genes for interleukin (IL)-1alpha, IL-1beta, IL-1alpha/beta, and IL-1
- 452 receptor antagonist shows that IL-1beta is crucial in turpentine-induced fever
- 453 development and glucocorticoid secretion. *J Exp Med* 1998, **187(9):** 1463-1475.
- 454
- 455 34. Coban C, Igari Y, Yagi M, Reimer T, Koyama S, Aoshi T, *et al.* Immunogenicity of
- 456 whole-parasite vaccines against Plasmodium falciparum involves malarial hemozoin
- 457 and host TLR9. *Cell Host Microbe* 2010, **7(1):** 50-61.
- 458
- 459 35. Martinon F, Petrilli V, Mayor A, Tardivel A, Tschopp J. Gout-associated uric acid
- 460 crystals activate the NALP3 inflammasome. *Nature* 2006, **440(7081):** 237-241.
- 461
- 462 36. Koedel U, Winkler F, Angele B, Fontana A, Flavell RA, Pfister HW. Role of
- 463 Caspase-1 in experimental pneumococcal meningitis: Evidence from pharmacologic
- 464 Caspase inhibition and Caspase-1-deficient mice. *Ann Neurol* 2002, **51(3):** 319-329.
- 465

- 466 37. Tomura M, Honda T, Tanizaki H, Otsuka A, Egawa G, Tokura Y, *et al.* Activated
467 regulatory T cells are the major T cell type emigrating from the skin during a
468 cutaneous immune response in mice. *J Clin Invest* 2010, **120**(3): 883-893.
469
470

METHODS

Mice

Female 8- to 12-week-old C57BL/6-background mice were used in this study. C57BL/6N mice were purchased from SLC (Shizuoka, Japan). Langerin-eGFP-DTR²⁸, CD11c-DTR²⁹, CD11c-YFP³⁰, LysM-DTR³¹, Rag2-deficient³², MasTRECK^{12, 13}, BasTRECK^{12, 13}, ALY/NscJcl-*aly/aly*¹¹, IL-1 α / β -deficient³³, IL-1R1-deficient³⁴, NLRP3-deficient³⁵, and caspase-1/11-deficient mice³⁶ were described previously. All experimental procedures were approved by the Institutional Animal Care and Use Committee of Kyoto University Graduate School of Medicine.

Human Subjects

Human skin biopsy samples were obtained from a nickel-reactive patch after 48 h from placement of nickel patch tests in patients with a previously proven allergic contact dermatitis. A biopsy of petrolatum-occluded skin was also obtained as a control. Informed consent was obtained under IRB approved protocols at the Icahn School of Medicine at Mount Sinai School Medical Center, and the Rockefeller University in New York.

Induction of contact hypersensitivity (CHS) response

Mice were sensitized on shaved abdominal skin with 25 μ l 0.5% (w/v) 1-fluoro-2,4-dinitrofluorobenzene (DNFB; Nacalai Tesque, Kyoto, Japan) dissolved in acetone/olive oil (4/1). Five days later, the ears were challenged with 20 μ l 0.3% DNFB. For adoptive transfer, T cells were magnetically sorted using auto MACS (Miltenyi Biotec, Bergisch Gladbach, Germany) from the draining LNs of sensitized mice and then transferred 1×10^7 cells intravenously into naïve mice.

Depletion of cutaneous DC subsets, macrophages, and neutrophils

To deplete all cutaneous DC subsets (including LCs), 6-week-old Langerin-DTR mice were irradiated (two doses of 550 Rad given 3 h apart) and were transferred with 1×10^7 BM cells from CD11c-DTR mice. Eight weeks later, 2 μ g diphtheria toxin (DT; Sigma-Aldrich, St. Louis, MO) was intraperitoneally injected. To selectively deplete LCs, irradiated Langerin-DTR mice were transferred with BM cells from C57BL/6 mice, and 1 μ g DT was injected. To selectively deplete dermal DCs, irradiated C57BL/6 mice were transferred with BM cells from CD11c-DTR mice, and 2 μ g DT was injected. For macrophage depletion,

irradiated C57BL/6 mice were transferred with BM cells from LysM-DTR mice and 800 ng DT was injected. For neutrophil depletion, 0.5 mg/body anti-Ly6G antibody (1A8, BioXCell, Shiga, Japan) were intravenously administered to mice 24 h before experiment.

Time-lapse imaging of cutaneous DCs, macrophages, and T cells

Cutaneous DCs were observed using CD11c-YFP mice. To label cutaneous macrophages *in vivo*, 5 mg TRITC-dextran (Sigma-Aldrich) was intravenously injected and mice were left for 24 h. At that time, cutaneous macrophages become fluorescent because they incorporated extravasated dextran. To label skin-infiltrating T cells, T cells from DNFB-sensitized mice were labeled with CellTracker Orange CMTMR (Invitrogen, Carlsbad, CA) and adoptively transferred. Keratinocytes and sebaceous glands were visualized with the subcutaneous injection of isolectin B4 (Invitrogen) and BODIPY (Molecular Probes, Carlsbad, CA), respectively. Mice were positioned on the heating plate on the stage of a two-photon microscope IX-81 (Olympus, Tokyo, Japan) and their ear lobes were fixed beneath a cover slip with a single drop of immersion oil. Stacks of 10 images, spaced 3 μm apart, were acquired at 1 to 7 min intervals for up to 24 h. To calculate T cell and DC velocities, movies from 3 independent mice were processed and analyzed using Imaris7.2.1 (Bitplane, South Windsor, CT) for each experiment.

Histology and immunohistochemistry

For histological examination, tissues were fixed with 10% formalin in phosphate buffer saline, and then embedded in paraffin. Sections with a thickness of 5 μm were prepared and subjected to staining with hematoxylin and eosin. For whole-mount staining, the ears were split into dorsal and ventral halves, and incubated with 0.5 M ammonium thiocyanate for 30 min at 37°C³⁷. Then the dermal sheets were separated and fixed in acetone for 10 min at -20°C. After treatment with Image-iT FX Signal Enhancer (Invitrogen), the sheets were incubated with anti-mouse MHC class II antibody (eBioscience, San Diego, CA) followed by incubation with secondary antibody conjugated to Alexa 488 or 594 (Invitrogen). The slides were mounted using a ProLong Antifade kit with DAPI (Molecular Probes) and observed under a fluorescent microscope (BZ-900, KEYENCE, Osaka, Japan). The number/size of DC clusters were evaluated in 10 fields of 1mm²/ ear and were scored according to the criteria shown in Supplementary Fig. 5a.

537

538 **Cell isolation and flow cytometry**

539 To isolate skin lymphocytes, the ear splits were put into digestion buffer
540 (RPMI supplemented with 2% fetal calf serum, 0.33 mg/ml of Liberase TL (Roche, Lewes,
541 UK), and 0.05% DNase I (Sigma-Aldrich)) for 1 hr at 37°C. After the incubation, the tissue
542 was disrupted by passage through a 70 µm cell strainer and stained with respective antibodies.
543 For analysis of intracellular cytokine production, cell suspensions were obtained in the
544 presence of 10 µg/ml of Brefeldine A (Sigma-Aldrich) and were fixed with Cytofix buffer,
545 permeabilized with Perm/Wash buffer (BD Biosciences) as per the manufacturer's protocol.
546 To stain cells, anti-mouse CD4, CD8, CD11b, CD11c, B220, MHC class II, F4/80, IFN-γ,
547 Gr1 antibodies and 7-amino-actinomycin D (7AAD) were purchased from eBioscience.
548 Anti-mouse CD45 antibody (BioLegend, San Diego, CA), anti-TCR-β antibody (BioLegend),
549 and anti-CD16/CD32 antibody (BD Biosciences) were purchased. Flow cytometry was
550 performed using LSRFortessa (BD Biosciences) and analyzed with FlowJo (TreeStar, San
551 Carlos, CA).

552

553 **Chemotaxis assay**

554 Chemotaxis was performed as described previously with some modifications³⁷. In brief, the
555 dermis of the ear skin was minced and digested with 2 mg/ml collagenase type II
556 (Worthington Biochemical, NY) containing 1 mg/ml hyaluronidase (Sigma-Aldrich) and 100
557 µg/ml DNase I (Sigma-Aldrich) for 30 min at 37°C. DDCs and macrophages were isolated
558 using auto-MACS. Alternatively, BM-derived DCs and macrophages were prepared. 1 x 10⁶
559 DCs were added to the 5 µm pore-size transwell insert (Corning, Cambridge, MA) and 5 x
560 10⁵ macrophages were added into the lower wells, and the cells were incubated at 37°C for
561 12 h. A known number of fluorescent reference beads (FlowCount fluorospheres, Beckman
562 Coulter, Fullerton, CA) were added to each sample to allow accurate quantification of
563 migrated cells in the lower wells by flow cytometry.

564

565 **Cell proliferation assay with CellTrace™ Violet**

566 Mice were sensitized with 25 µl 0.5% DNFB or 7% trinitrochlorobenzene (Chemical Industry,
567 Tokyo, Japan). Five days later, T cells were magnetically separated from the draining LNs of
568 each group, and labeled with CellTrace™ Violet (Invitrogen) as per the manufacturer's
569 protocol. Ten million T cells were adoptively transferred to naïve mice, and the ears were

challenged with 20 μ l of 0.5% DNFB. Twenty-four hours later, ears were collected and analyzed by flow cytometry.

In vitro differentiation of DCs, M1 and M2-phenotype macrophages from BM cells

BM cells from the tibias and fibulas were plated 5×10^6 cells/ 10cm dishes on day 0. For DC differentiation, cells were cultured at 37°C in 5% CO₂ in cRPMI medium (RPMI supplemented with 1% L-glutamine, 1% Hepes, 0.1% 2ME and 10% fetal bovine serum) containing 10 ng/mL GM-CSF (Peprotech, Rocky Hill, NJ). For macrophages differentiation, BM cells were cultured in cRPMI containing 10 ng/mL M-CSF (Peprotech). Medium was replaced on days 3 and 6 and cells were harvested on day 9. To induce M1 or M2 phenotypes, cells were stimulated for 48 h with IFN- γ (10 ng/mL; R&D Systems, Minneapolis, MN) or with IL-4 (20 ng/mL; R&D Systems), respectively.

In vitro IL-1 α stimulation assay of dermal macrophages

Dermal macrophages were separated from IL-1 α / β -deficient mice³³ to avoid pre-activation during cell preparations. Ear splits were treated with 0.25% trypsin/EDTA for 30 min at 37°C to remove epidermis and then minced and incubated with collagenase as previously described. CD11b⁺ cells were separated using MACS and 2×10^5 cells/well were incubated with or without 10 ng/ml IL-1 α (R&D systems) in 96-well plate for 24 h.

Blocking assay

For LFA-1 blocking assay, mice were intravenously injected with 100 μ g anti-LFA-1 neutralizing antibody, KBA, 12-14 h after challenge with 20 μ l 0.5% DNFB. For IL-1R blocking, mice were subcutaneously injected with 10 μ g IL-1R antagonist (PROSPEC, East Brunswick, NJ) 5 h before challenge. For blocking of CXCR2, mice were intraperitoneally treated with 50 μ g CXCR2 inhibitor SB265610¹⁶ (Tocris Bioscience, Bristol, UK) 6 h before and at hapten painting.

Quantitative PCR analysis

Total RNA was isolated using an RNeasy Mini kit (Qiagen, Hilden, Germany). cDNA was synthesized using a PrimeScript RT reagent kit (TaKaRa, Ohtsu, Japan) with random hexamers as per the manufacturer's protocol. Quantitative PCR was carried out with a LightCycler 480 using a LightCycler SYBR Green I master (Roche) as per the

manufacturer's protocol. The relative expression of each gene was normalized against that of Gapdh. Primer sequences are shown in Supplementary Table 2.

Microarray analysis

Total RNA was isolated using the RNeasy Mini Kit (Qiagen) as per the manufacturers' protocol. An amplified sense-strand DNA product was synthesized by the Ambion WT Expression Kit (Life Technologies, Gaithersburg, MD), and was fragmented and labeled by the WT Terminal Labeling and Controls Kit (Affymetrix, Santa Clara, CA), and was hybridized to the Mouse Gene 1.0 ST Array (Affymetrix). We used the robust multi-array average algorithm for log transformation (log2) and normalization of the GeneChip data. Microarray data have been deposited in NCBI-GEO under accession number GSE53680.

General experimental design and statistical analysis

For animal experiments, a sample size of three to five mice per group was determined on the basis of past experience in generating statistical significance. Mice were randomly assigned to study groups and no specific randomization or blinding protocol was used. Sample or mouse identity was not masked for any of these studies. Statistical analyses were performed using Prism software (GraphPad Software Inc.). Normal distribution was assumed a priori for all samples. Unless indicated otherwise, an unpaired parametric *t*-test was used for comparison of data sets. In cases in which the data point distribution was not Gaussian, a nonparametric *t*-test was also applied. *P* values of less than 0.05 were considered significant.

Figure Legends

Figure 1: DC–T cell cluster formation is responsible for epidermal eczematous conditions.

(a) Clinical manifestations of allergic contact dermatitis in human skin 48 h after a patch test with nickel. Scale bar = 200 μ m. (b) Hematoxylin and eosin, anti-CD3, and anti-CD11c staining of the human skin biopsy sample from an eczematous lesion. Asterisks and arrowheads denote epidermal vesicles and dDC–T cell clusters, respectively. Scale bar = 250 μ m. (c) Sequential images of leukocyte clusters in the elicitation phase of CHS. White circles represent DC (green) and T cell (red) dermal accumulations. Scale bar = 100 μ m. (d) A high magnification view of DC–T cell cluster in Fig.1c. Scale bar = 10 μ m. (e) Interstitial edema of the epidermis overlying DC–T cell cluster in the dermis. Keratinocytes (red) are visualized with isolectin B4. The right panel shows the mean distance between adjacent keratinocytes above (+) or not above (–) DC–T cell cluster (n=20, each). Scale bar = 10 μ m. (f) Ear swelling 24 h after CHS in subset-specific DC-depletion models (n = 5, each). *, $P < 0.001$. (g) The number (left) and the % frequency (right) of IFN- γ producing T cells in the ear 18 h after CHS with or without dDC-depletion (n = 5, each). *, $P < 0.05$.

Figure 2: Antigen-dependent T cell proliferation in DC–T cell clusters. (a) T cell proliferation in the skin. CD4⁺ and CD8⁺ T cells from DNFB- (red) or TNCB- (blue) sensitized mice were labeled with CellTrace™ Violet and transferred. The dilutions of tracer in the challenged sites were examined 24 h later. (b) Conjugation time of DNFB- (red, n = 160) or TNCB-sensitized (blue, n = 60) T cells with dDCs 24 h after DNFB challenge. *, $P < 0.05$. (c) Sequential images of dividing T cells (red) in DC–T cell clusters. Green represents dDCs. Arrowheads represent a dividing T cell.

Figure 3: LFA-1 is essential for the persistence of DC–T cell clustering and for T cell activation in the skin. (a) DC (green) and T cell (red) clusters in the DNFB-challenged site before (0 h) and 9 h after KBA or isotype-matched IgG treatment. Scale bar = 100 μ m. (b) Fold changes of T cell velocities in DNFB-challenged sites after KBA or control IgG treatment (n = 30, each). (c) Ear swelling 24 h after KBA (red) or control IgG (black) treatment with DNFB challenge (n = 5, each). (d and e) IFN- γ production by CD8⁺ T cells (d) and the number of IFN- γ producing cells in CD4⁺ or CD8⁺ populations (e) in KBA (red) or control IgG (black) treated mice (n = 5, each). DNFB-sensitized mice were treated with KBA or control IgG 12 h after DNFB challenge and the skin samples were obtained 6 h later. *, P

< 0.05.

Figure 4: Macrophages are essential for DC cluster formation. **(a)** Score of DC cluster number 24 h and 48 h after DNFB application in sensitization (red) or elicitation (green) phase of CHS (n=4, each). **(b)** Score of DC cluster number in non-treated (NT) mice and DNFB-applied C57BL/6 (WT), Rag2-deficient, aly/aly, MasTRECK, BasTRECK, LysM-DTR, and 1A8-treated mice (n=4, each). *, $P < 0.05$. **(c)** DC clusters observed in LysM-DTR BM chimeric mice with or without DT-treatment. Scale bar = 100 μ m. **(d)** Ear swelling 24 h after DNFB application in LysM-DTR BM chimeric mice with (red) or without (black) DT-treatment (n = 5, each). **(e)** The number (left) and the % frequency (right) of IFN- γ producing CD8⁺ T cells in the ear 18 h after DNFB application in LysM-DTR BM chimeric mice with (red) or without (black) DT-treatment (n = 5, each). *, $P < 0.05$.

Figure 5: Macrophages mediate perivascular DC cluster formation. **(a)** A distribution of dDCs (green) in the steady state (left) and in the elicitation phase of CHS (right). The white circles show DC clusters. Sebaceous glands visualized with BODIPY (green) are indicated by arrows. Blood vessels, yellow/red; macrophages, red. **(b)** A high magnification view of perivascular DC cluster. Scale bar = 100 μ m. **(c)** Sequential images of dDCs (green) and macrophages (red) in the elicitation phase of CHS. The white dashed line represents the track of a DC. **(d)** Chemotaxis assay. % input of dDCs transmigrating into the lower chamber with or without macrophages prepared from the skin.

Figure 6: IL-1 α upregulates CXCR2 ligands expression in M2-phenotype macrophages to form DC clusters. **(a)** Scores of DC cluster numbers in NT or 24 h after hapten-painted sites in WT, IL-1R-, NALP3-, or caspase 1 (Casp1)-deficient mice (n=4, each). **(b)** Scores of DC cluster numbers in NT or 24 h after hapten-painted sites in isotype control IgG, anti-IL- α antibody, anti-IL-1 β antibody, IL-1R antagonist, or pertussis toxin (Ptx)-treated mice (n=4, each). **(c, d)** Ear swelling 24 h after DNFB application (c) and the number (left) and the % frequency (right) of IFN- γ producing CD8⁺ T cells in the ear 18 h after DNFB application (d) in mice that lack both IL-1 α and IL-1 β (red) and WT (black) mice (n = 5, each) which were adoptively transferred with DNFB-sensitized T cells. *, $P < 0.05$. **(e, f)** Relative amount of *Il1r1* and *Cxcl2* mRNA expression. Quantitative RT-PCR analysis of mRNA obtained from M1 or M2-phenotype macrophages (e), cultured with (+) or without (-)

693 IL-1 α (f) (n=4, each). (g) Scores of DC cluster numbers in NT or 24 h after hapten-painted
694 sites in the presence (SB265610) or absence (vehicle) of a CXCR2 inhibitor (n=4, each). *, P
695 < 0.05. (h, i) Ear swelling 24 h after DNFB application (h) and the number (right) and the %
696 frequency (left) of IFN- γ producing CD8⁺ T cells 18 h after DNFB application (i) with (red)
697 or without (black) SB265610-treatment (n = 5, each). *, P < 0.05.

Figure 1

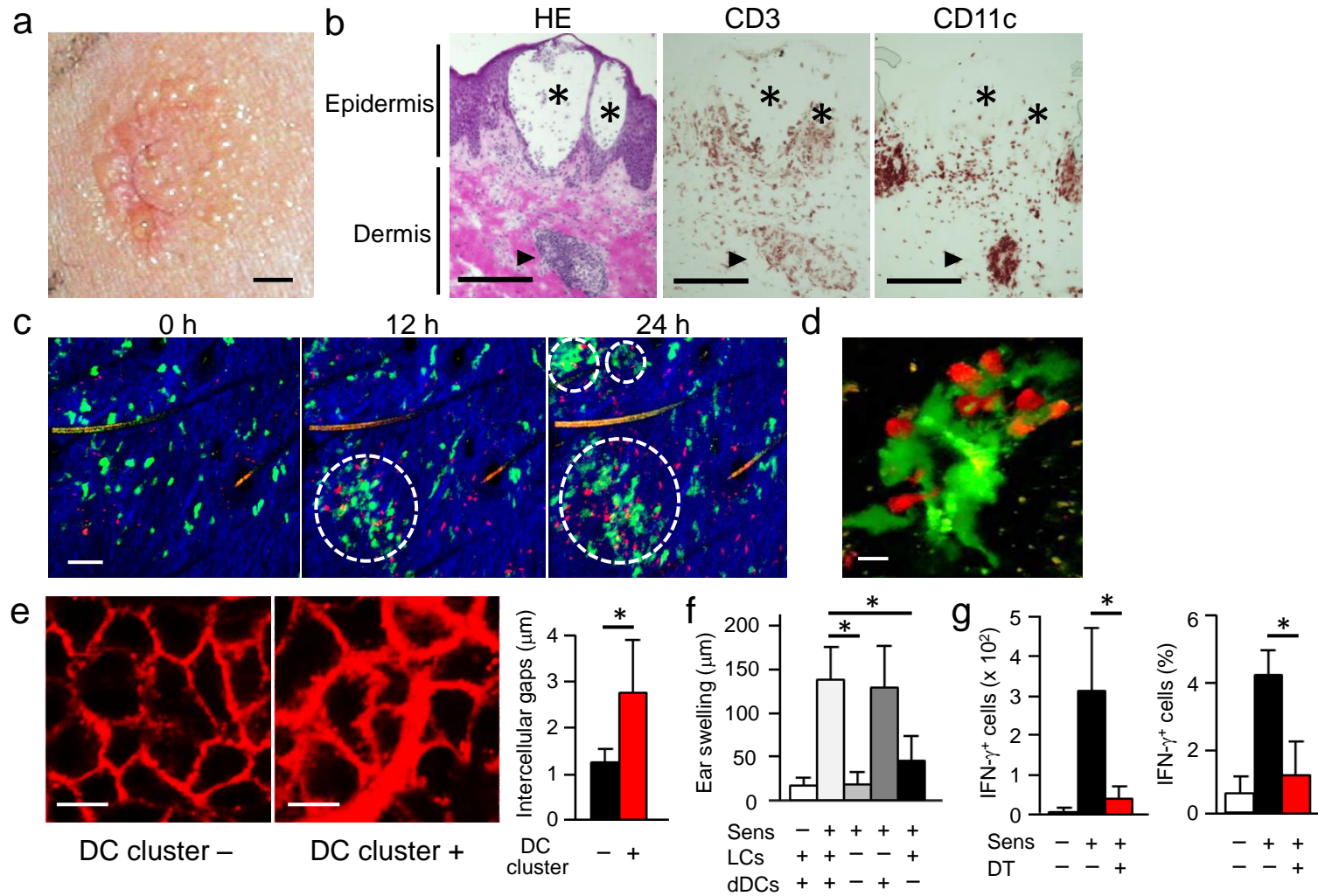


Figure 2

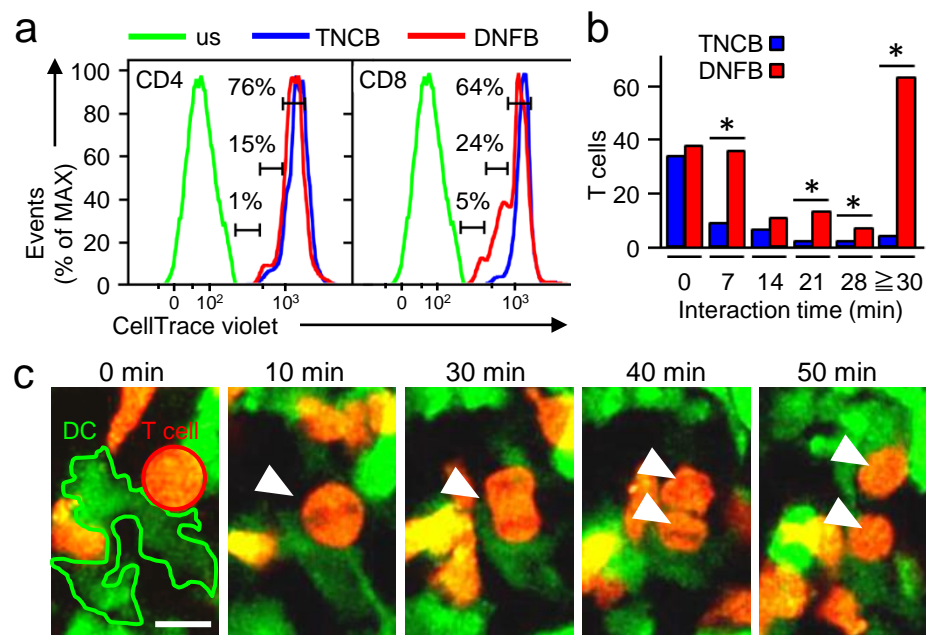


Figure 3

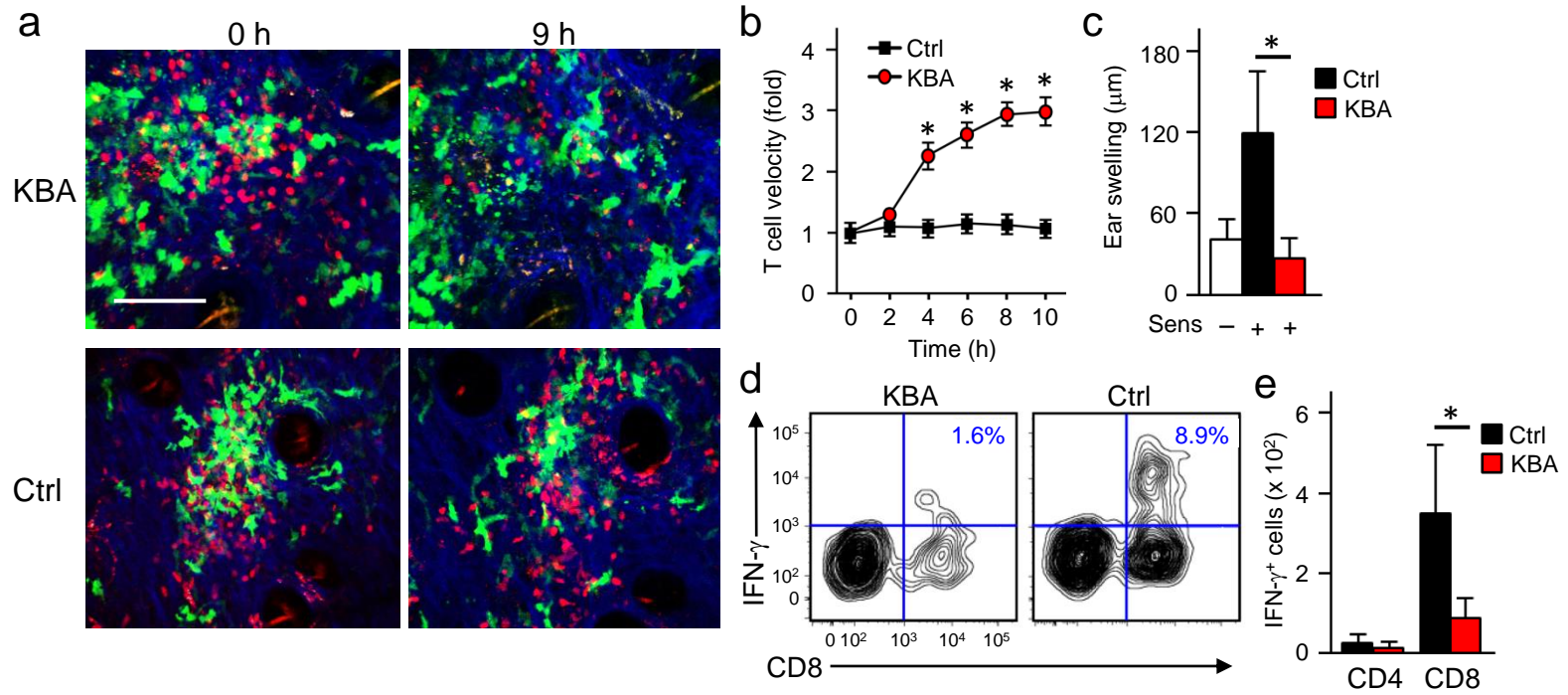


Figure 4

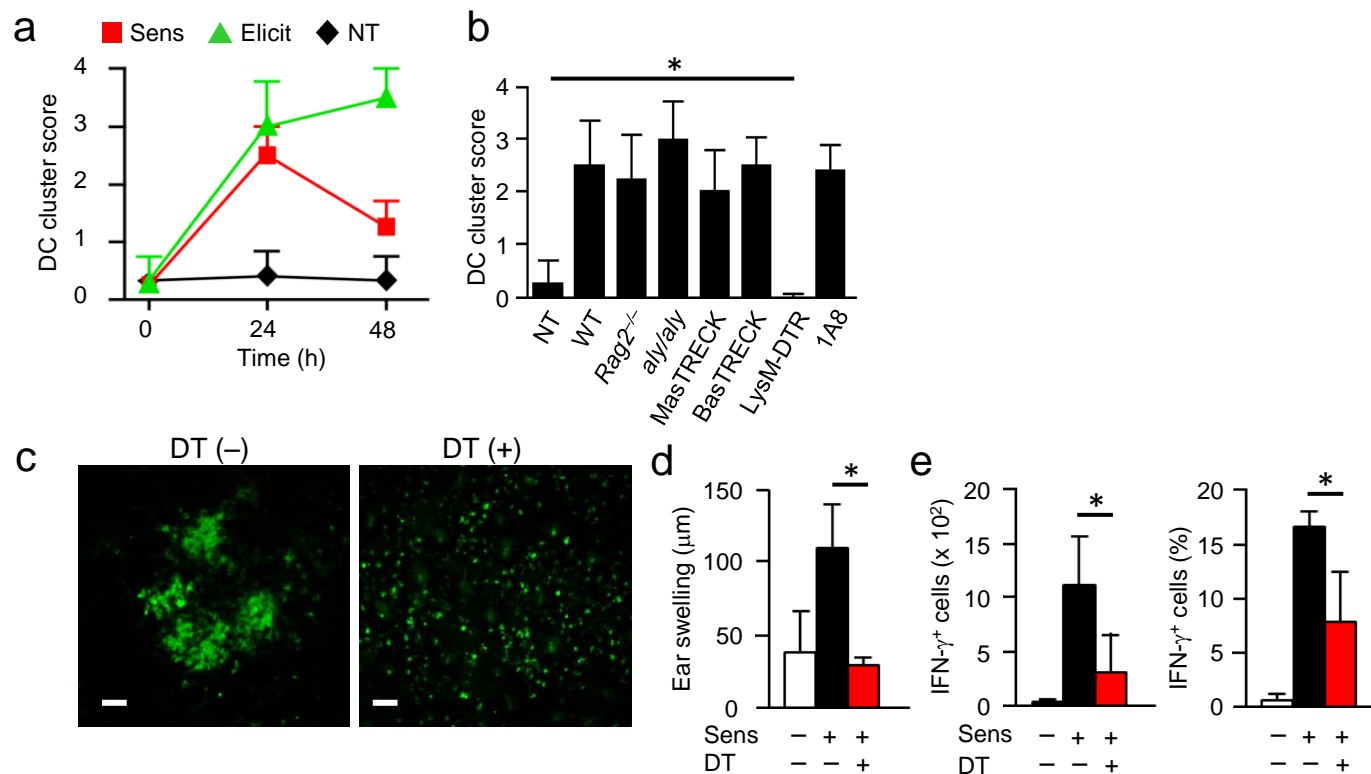


Figure 5

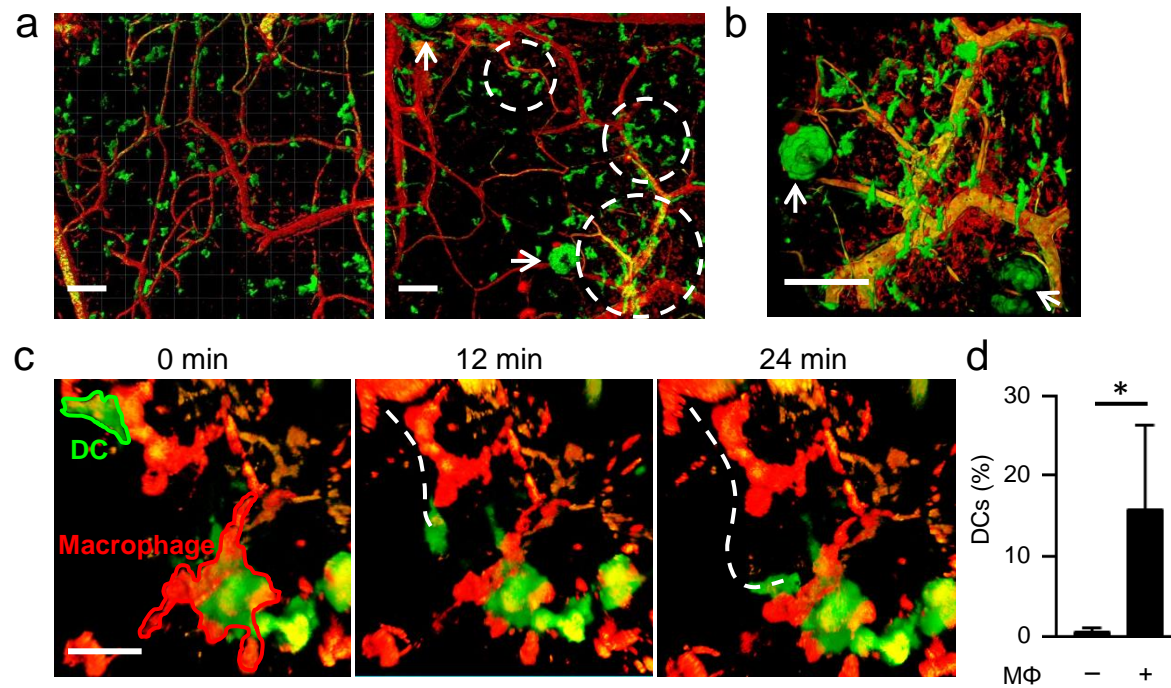
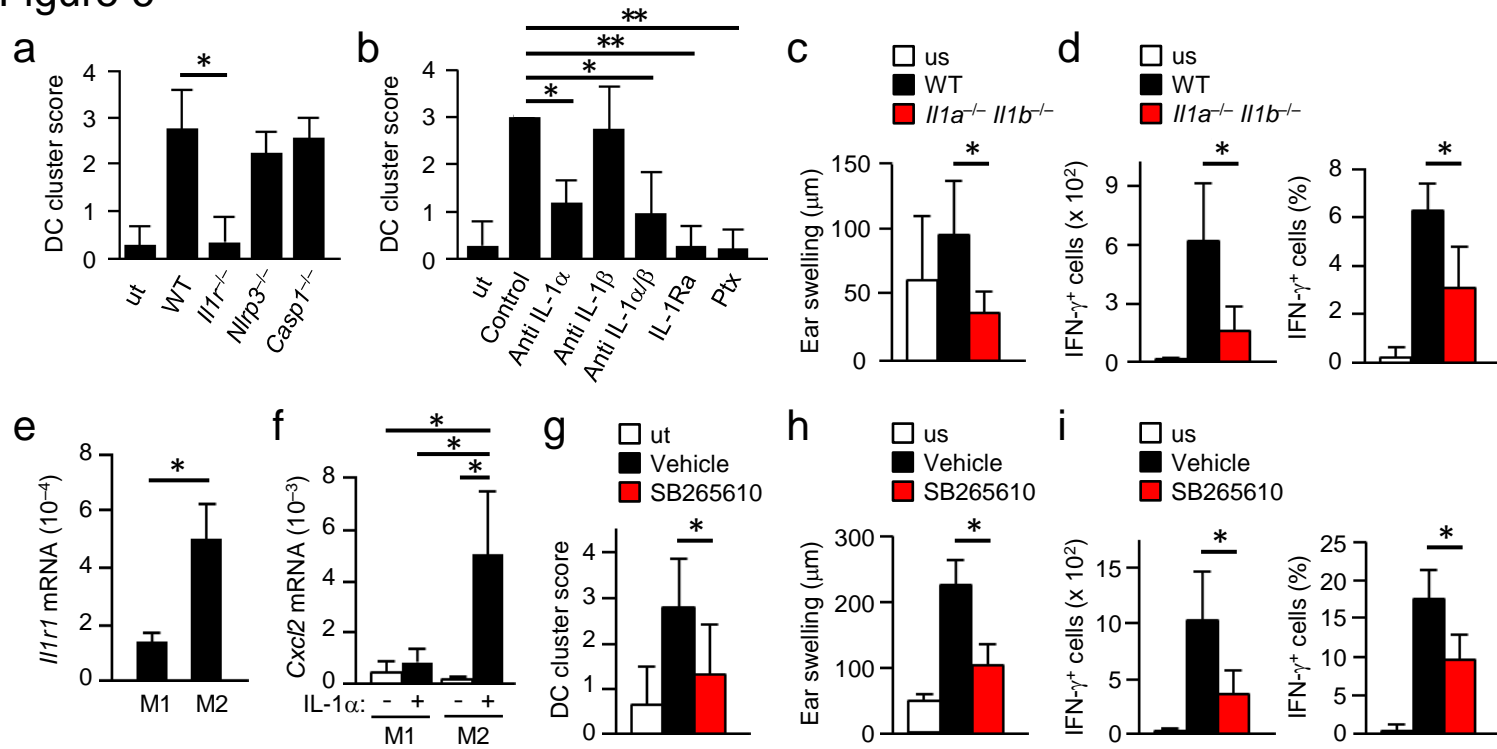
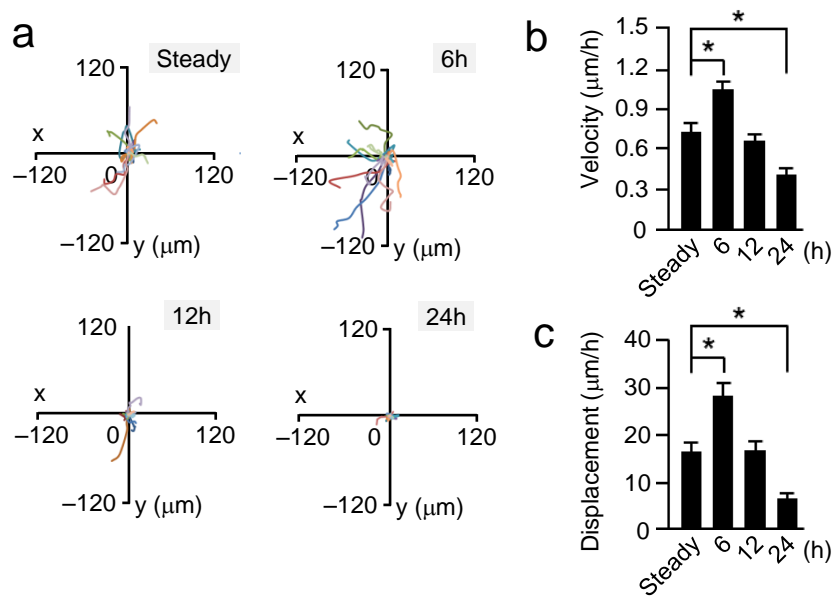


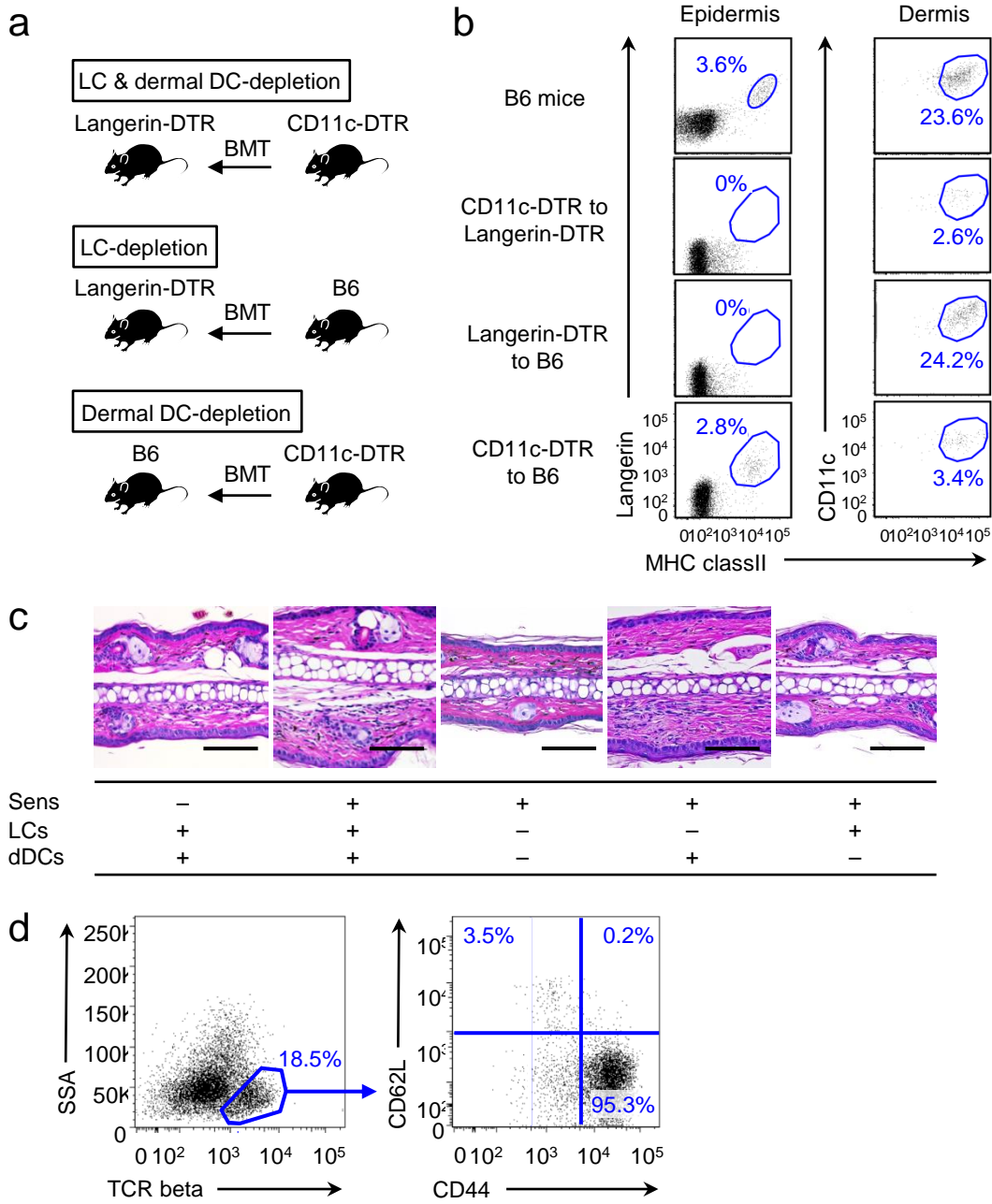
Figure 6



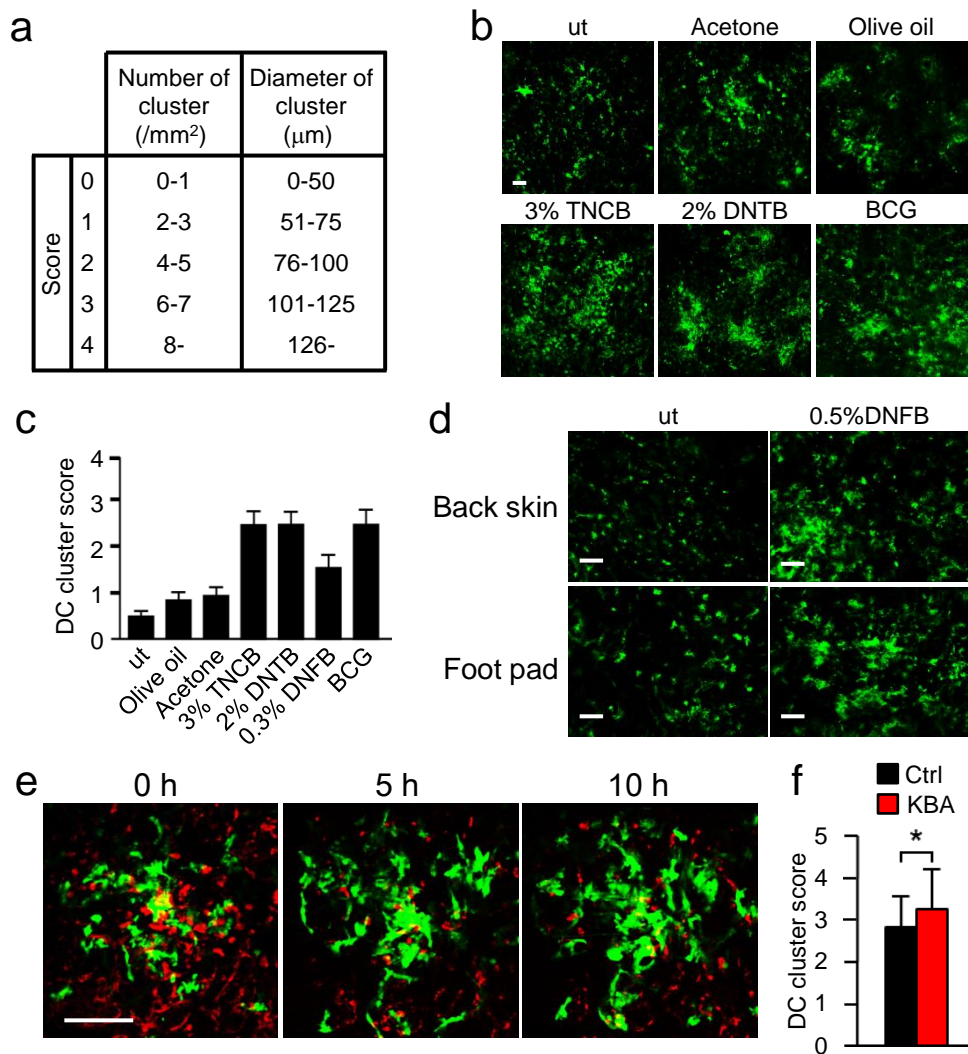
Supplementary Figure 1



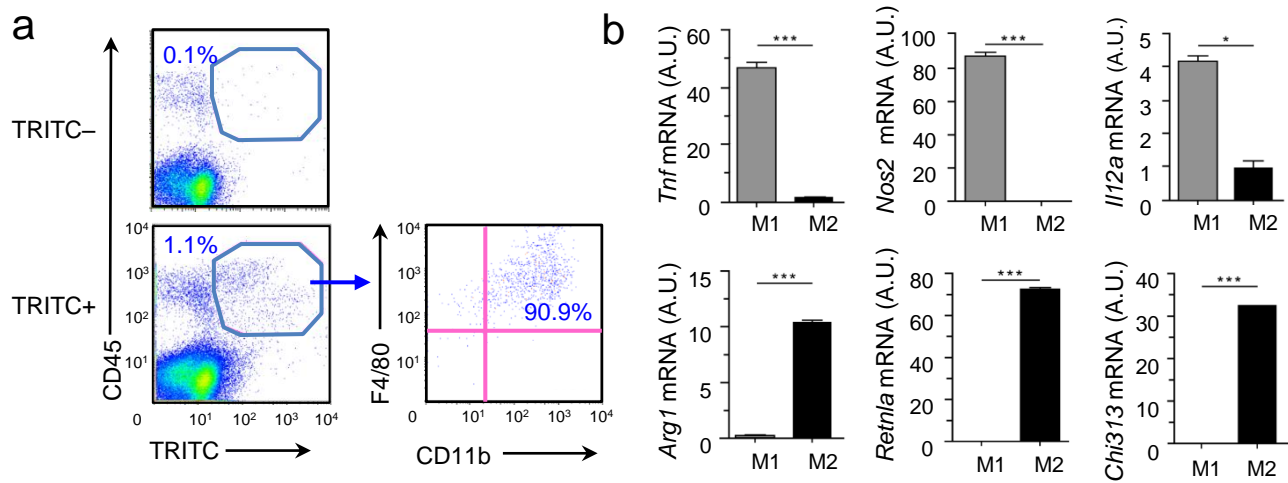
Supplementary Figure 2



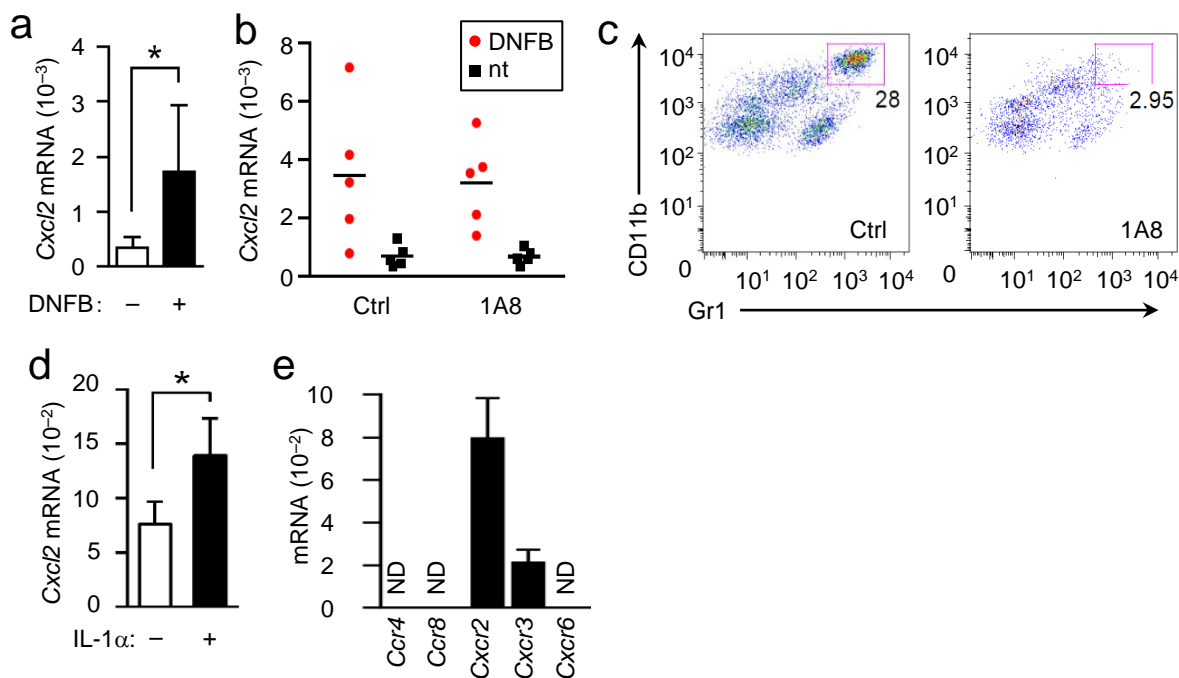
Supplementary Figure 3



Supplementary Figure 4



Supplementary Figure 5



Supplementary Figure 6

